

Effects of different ventilation modes on thermal comfort and contaminant removal effectiveness in ship cabin

Lei Guo*, Libo Dai, Jiajie Peng
Marine Design & Research Institute of China, Shanghai 200011, China

ABSTRACT

Ships have cabins with compact spaces, dense personnel, and complex hull structures, and the air conditioning and ventilation design faces significant challenges. To study the thermal comfort and contaminant removal effectiveness and other indexes when different ventilation modes are used in ship cabins and to guide the design of air conditioning and ventilation in ship cabins, the computational fluid dynamics method was compared and verified with experiments, and then a numerical computation model of the ship's academic hall was established. Three ventilation design schemes for the ship's academic hall were compared and analyzed, and the results show that the optimized displacement ventilation has the best thermal comfort indexes, the highest contaminant removal effectiveness, and the thermal comfort indexes meet the standard requirements. The results provide a reference for selecting and designing ship cabin air conditioning and ventilation.

Keywords: Mixed ventilation, displacement ventilation, computational fluid dynamics, ship cabin airflow, thermal comfort indexes, contaminant removal effectiveness, ventilation design optimization

1. INTRODUCTION

Ensuring optimal air quality and thermal comfort inside ship cabins is crucial to modern ship design, especially for high-end ships such as military, business, and luxury cruise ships. However, such ships' heating, ventilation and air conditioning (HVAC) designs are more complex due to compact space, limited floor height, and dense personnel. In addition to the need to meet the crew's thermal comfort needs, due to the diverse functions of ship cabins, the types of contaminants in ship cabins are also diverse¹. The requirements for controlling the concentration of contaminants or eliminating contaminants are also increasing, and contaminant propagation control and exclude methods have also become an essential part of ship cabin HVAC design.

Traditional ship cabin HVAC design mainly relies on empirical formulas for theoretical calculations, however, the final implementation effect is unpredictable, so it is challenging to adapt to the increasing design requirements. With the development of the computational fluid dynamics (CFD) method, ship cabin HVAC design has become more accurate, convenient and fast, reducing the design cycle and research and development costs, many scholars and designers have carried out research and design work in this area, Acar² focused on the HVAC performance of a dorm compartment on a naval surface ship and numerical analyses were conducted for different scenarios to optimize the cooling effect by changing the location of the air outlets, and the results also showed that a higher number of air changes does not imply better thermal comfort. Shi³ investigated the effects of different air supply parameters on comfort and anti-fog characteristics using CFD simulation methods, it was found that the best thermal comfort and fog reduction effects for the driver are provided by the "Down-supply up-return type vertical jet" air supply method. Zhang⁴ analyzed two different air supply modes for luxury cruise air-conditioning cabins and concluded that the mode of up-supply up-return is more effective in controlling cabin temperature and air velocity. Khalil⁵ examined how variations in the location, size, and number of air supply and exhaust grilles, along with changing boundary conditions, affect thermal comfort in a cruise ship hall. Sun⁶ developed a physical model for implementing a cooling ceiling and fresh air system in the ship conference room and analyzed the optimal fresh air supply mode when using a cooling ceiling. The study found that displacement ventilation offers the best comprehensive performance indicators. Liu⁷ analyzed the original air-conditioning system in the cabin and proposed three improved air-conditioning systems, and the results showed that the under-supply air-conditioning system was 2-4°C lower than that of the original air-conditioning system.

*guolei@maric.com.cn

However, these studies mainly focus on a single ventilation mode, and their optimization is only for the adjustment of air vents, and there are fewer studies for the exclusion of contaminants. Currently, commonly used ventilation modes can be categorized into mixed ventilation, displacement ventilation, and local ventilation⁸. In mixed ventilation, the air supply temperature is calculated according to the cooling and heating loads, and the air is usually sent into the cabin at high velocity, the air jet is fully mixed with the air inside the cabin, and the occupied zone is ventilated by relying on the air jet or the return flow caused by the air jet. In displacement ventilation, the air supply vents are provided at or near the floor, and treated air is fed through the vents into the lower regions of the cabin at a temperature slightly lower than that required for the occupied zone of the cabin and at a lower velocity, return or exhaust vents are provided at or near the ceiling. In local ventilation, air is supplied to only a portion of the cabin or areas of frequent activity, and the treated air is usually delivered directly to the vicinity of the personnel to create a comfortable air environment or reduce the concentration of contaminant.

In order to improve the thermal comfort and contaminant removal efficiency of ship cabins, it is necessary to analyze and compare the CFD simulation for different design schemes of ship cabin air conditioning and ventilation. In this paper, we first take an experimental cabin as an example to verify the simulation method, and then numerically simulate different ventilation schemes for a ship's academic hall and optimize the design of air conditioning and ventilation based on the CFD simulation results to improve thermal comfort and contaminant exclusion efficiency.

2. METHOD

2.1 CFD method

The governing equations for heat transfer in air flow include the continuity, momentum, energy, and component equations, which can be expressed in the following generalized form:

$$\frac{\partial(\rho\phi)}{\partial t} + \text{div}(\rho\mathbf{u}\phi) = \text{div}(\Gamma\text{grad}\phi) + S \quad (1)$$

The exact form of each term in equation (1) can be found in Reference⁹.

In this paper, the finite volume method based on structured adaptive mesh is used to solve the Reynolds-averaged N-S equations. The local mesh optimization technique is used to deal with the boundary of the complex object. The boundary layer effect is dealt with using the two-scale wall function model, and a k-ε turbulence model based on the Reynolds-averaged N-S equations is used to deal with turbulence, which has been widely used in engineering. This model is widely used in the engineering field, and its basic principle is to introduce the turbulent kinetic energy k equation and the turbulent kinetic energy dissipation rate ε equation to form a k-ε two-equation model to solve the turbulent flow field. The spatial discretization adopts the difference format with second-order accuracy, in which the convective term adopts the windward format, the diffusive term utilizes the central difference discretization, the time discretization adopts the implicit Eulerian format, and the coupled velocity-pressure equations are solved by the SIMPLE-like method. The discrete coordinate model is utilized to solve the radiative heat transfer problem.

2.2 Thermal comfort and contaminant removal effectiveness

In this paper, the assessment metrics such as Predicted Mean Vote (*PMV*), Predicted Percentage Dissatisfaction (*PPD*), Draft Rate (*DR*), and Percentage Dissatisfaction of Vertical Temperature Difference (*PD*) are used for the assessment of thermal comfort^{10,11}.

Contaminant removal effectiveness (*CRE*) is defined as:

$$CRE = \frac{c_e - c_s}{c_{mean} - c_s} \quad (2)$$

where c_e is the exhaust air contaminant concentration, c_s is the supply air contaminant concentration and c_{mean} is the spatially averaged concentration.

The local air quality index (*LAQI*) indicates the efficiency of the ventilation system in removing contaminated air from a given point:

$$LAQI = \frac{c_e}{c} \quad (3)$$

where c is the concentration of a contaminant at a given point.

For an ideal mixed ventilation system, the CRE is 1. For other systems, values above 1 indicate good contaminant removal effectiveness and below 1 indicate poor contaminant removal effectiveness.

2.3 Displacement ventilation design approach

There are two commonly used methods for designing displacement ventilation to safeguard the thermal comfort of people in the room, the first is the REHVA method¹², which is based on an experimental approach and assumes that the temperature distribution between the floor and the ceiling is linear. The second is the ASHRAE method¹³, based on a validated CFD program developed for typical American buildings, the method assumes that the temperature is linearly distributed in the head and foot range of the human body. Detailed calculation steps and equations are given in References^{12,13}.

Both methods are designed and calculated to determine the air supply and air temperature based on the predicted vertical temperature distribution, while in reality, the temperature distribution depends on the type and location of the heat source, the wall characteristics, the height of the space and the amount of air supply, the type and location of the air distributor, etc., and both methods are unable to take into account the effects of all parameters. The ASHRAE method considers relatively more parameters that can influence the vertical temperature distribution, but the method was developed for typical U.S. buildings and the authors have limited the scope of application of the method. It is necessary to validate and improve the design using methods such as CFD simulation if it is applied to more complex environments or different cabins.

3. VALIDATION OF CFD METHOD

In this paper, the displacement ventilation experimental room of Li^{14,15} is used as an example for CFD simulation and compared with experimental measurements to verify the accuracy of the computation method. Figure 1 shows the model of the experimental room, and Table 1 gives the dimensions and locations of the experimental room, as well as the heat source, supply air inlet, and exhaust air outlet. It should be noted that the heat source in the experiment consists of 24 bulbs, each with a thermal power of 25 W and a total heat capacity of 600 W, the main frame is an aluminum mesh filled with aluminum flakes, which is intended to distribute the heat load uniformly and to reduce the short-wave radiation from the heat source to the wall surface, and thus the heat source is similar to a porous medium. It is not easy to model this complex structure and set boundary conditions in numerical simulation, so in this study, the heat source is considered a solid with a volumetric heat generation of 600 W.

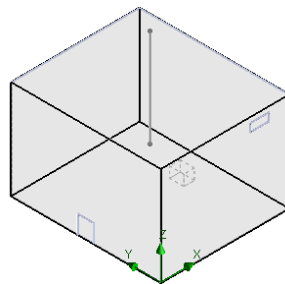


Figure 1. Experimental room model.

Table 1. Experimental room size and location.

Item	Width	Length	Height	Location		
	$\Delta x/m$	$\Delta y/m$	$\Delta z/m$	x/m	y/m	z/m
Room	3.6	4.2	2.75	1.8	2.1	1.375
Heat source	0.3	0.4	0.3	2.7	2.1	0.25
Air inlet	0	0.45	0.5	0	2.1	0.25
Air outlet	0.525	0	0.22	2.7825	0	2.5

In this paper, CFD simulations have been carried out using discrete ordinate (DO) radiation model, discrete transfer (DT) radiation model and no radiation model and compared with experimental values, and the results are shown in Figure 2a, where the vertical axis is the ratio of the height of the measurement point to the height of the room, and the horizontal axis is the difference between the temperature of the measurement point (T) and the temperature of the supply air (T_i). It can be seen that the deviation between the experiment and CFD is most significant when radiation is not taken into account, which indicates that it is necessary to take into account the radiation in the simulation of displacement ventilation and that the DO radiation model is closer to the experiment so that the DO radiation model can get more accurate results. The deviation between the experiment and CFD using the DO radiation model is shown in Figure 3b, where the CFD results underestimate the temperatures near the floor and ceiling, and the temperature changes near the ceiling are more complicated in the experiment and the reasons for these deviations may be related to the assumptions about the heat source settings, the distribution of the velocity of the air supply inlet, and the temperatures of the ceiling and floor surfaces. Overall, the agreement between the CFD and experiment is quite good, with average and maximum deviations of 2.8% and 12.3% in the temperature scale, respectively, which verifies the accuracy of the simulation method and allows for subsequent simulations in the ship cabin.

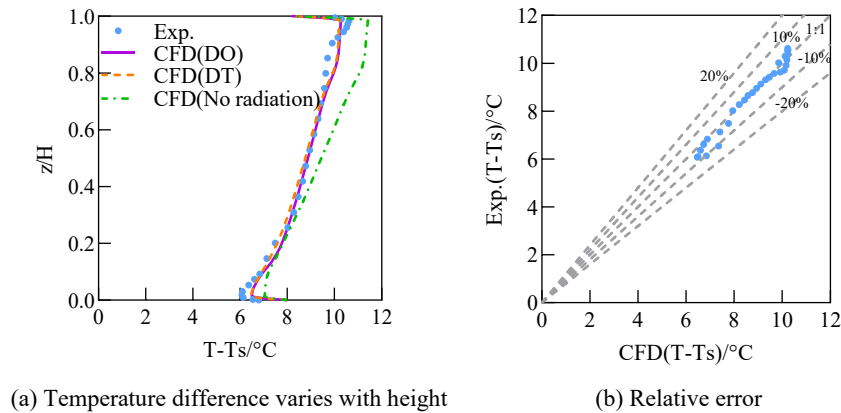


Figure 2. Comparison of experimental and CFD simulation results.

4. RESULTS AND DISCUSSION

The ship’s cabin studied in this paper is a ship’s academic hall, which has a width of 9.2 m, a length of 10.89 m, and a height from 2.08 m to 2.76 m, and the cabin arrangement is shown in Figure 3.

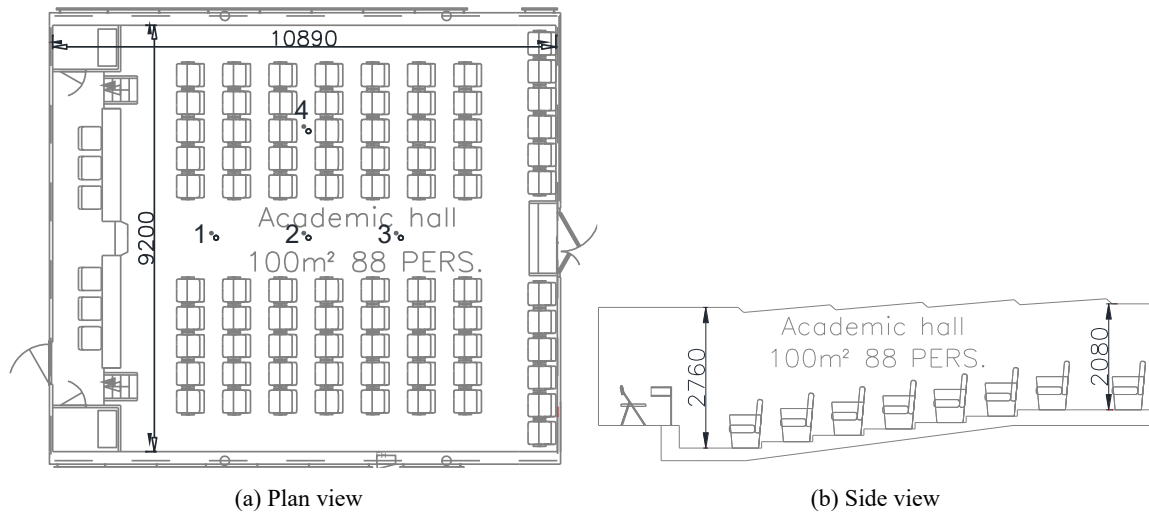


Figure 3. Layout of the academic hall.

The CFD numerical simulation model established according to the layout of the academic hall is shown in Figure 4.

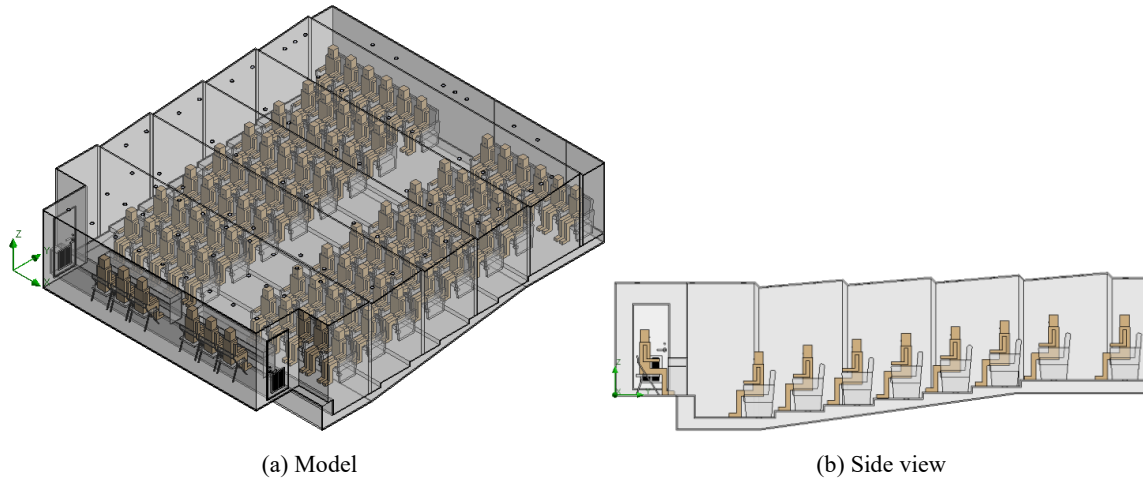


Figure 4. Model of the academic hall.

The academic hall summer design conditions for the ambient temperature of 35°C, the indoor temperature of 26°C, the fresh air ratio of 50%, and the heat transfer to the cabin are calculated according to the equations presented in the standard¹⁶, bulkheads, ceilings, and floors heat gaining for 2330 W, human bodies heat generation for 4840 W, lighting heat generation for 800 W.

Firstly, the mixed ventilation design of the academic hall was carried out, as shown in Figure 5a. The design process refers to the standard, and it can be determined that the air supply volume of the chamber is 4400 m³/h, a total of 18 air distributors are set up, the air is returned by the grilles on both sides of the podium door, the exhaust grilles located at the ceiling above the last row of seats has an exhaust volume of 900 m³/h. The air supply temperature for mixed ventilation is 20.5°C. In addition, personnel breathing is defined as a contaminant for tracking, and the breathing volume of each person is 0.72 m³/h.

In the displacement ventilation design, as shown in Figure 5b, the air conditioning duct sends air to the plenum chamber under the cabin. The air supply column is set under the seats. However, the seat air supply column cannot be set at the podium due to the pipeline arrangement and other reasons, so the front of the academic hall retains two air distributors, and the door grilles on both sides are used as the return air vents. Four air exhaust grilles are still on the top of the last row of seats.

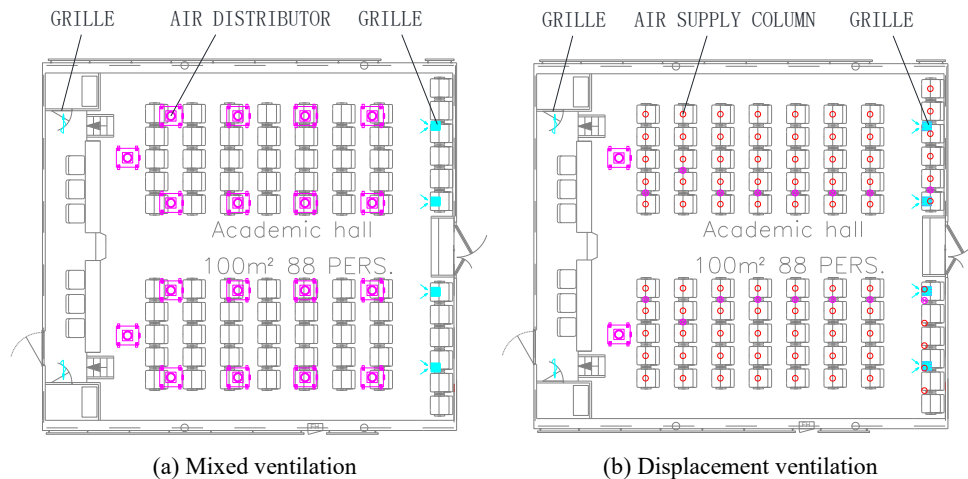


Figure 5. Mixed and displacement ventilation design.

In this study, two methods were used for the preliminary design of displacement ventilation. When using the REHVA method, it is assumed that the minimum design temperature $T_f=25^\circ\text{C}$, the maximum design temperature $T_h=27^\circ\text{C}$, and the height of the activity area of the cabin $h=1.95$ m, the seat air supply volume $q_v=4100$ m³/h and the air supply temperature

$T_s=22.1^\circ\text{C}$ are calculated according to the design guide¹². When using the ASHRAE method, assuming that the minimum design temperature $T_h=26^\circ\text{C}$, $\Delta T_h=1.5^\circ\text{C}$, the seat air supply $q_v=4000\text{ m}^3/\text{h}$ and air supply temperature $T_s=23.6^\circ\text{C}$ can be obtained according to the design steps described in the report¹³. It should be noted, Chen noted in his report that the data source of his computation model is a typical American building with room heights of 2.43-5.5 m, air changes of 2-15 times, unit area cooling loads of 21-120 W/m^2 , $0.08 \leq Q_{oe}/\Phi_{tot} \leq 0.68$, $0 \leq Q_l/\Phi_{tot} \leq 0.43$, and $0 \leq Q_{ex}/\Phi_{tot} \leq 0.92$. There are still some differences between the academic hall studied in this paper and the computation model in the ASHRAE method, in addition, considering that the cabin needs to arrange two air distributors as a supplement, this study is based on the computation results of the two methods, firstly, to determine the seat air supply volume $q_v=4000\text{ m}^3/\text{h}$, and then use different air supply temperatures to carry out CFD simulations, and take the average temperature of the occupied zone T_o as the computation target, to get the optimal displacement ventilation air supply temperature. The average temperature of the occupied zone with the air supply temperature changes as shown in Figure 6, and the average temperature of the occupied zone is 25.9°C when the air supply temperature is 22.0°C . Therefore, the air supply temperature of the displacement ventilation in the academic hall is determined to be $T_s=22.0^\circ\text{C}$. The air supply temperature of the displacement ventilation is increased by 1.5°C compared with that of the mixed ventilation, and the air-conditioning load of the academic hall in the case of the mixed ventilation is 48 kW, while the displacement ventilation operates at a lower load of only 41 kW, which is a 15% reduction in air conditioning load.

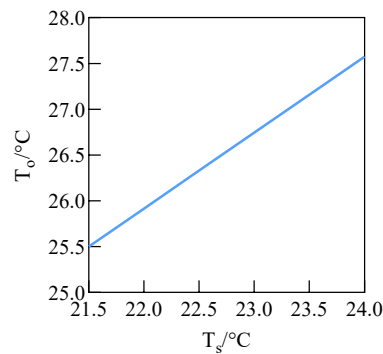


Figure 6. Average temperature of the occupied zone.

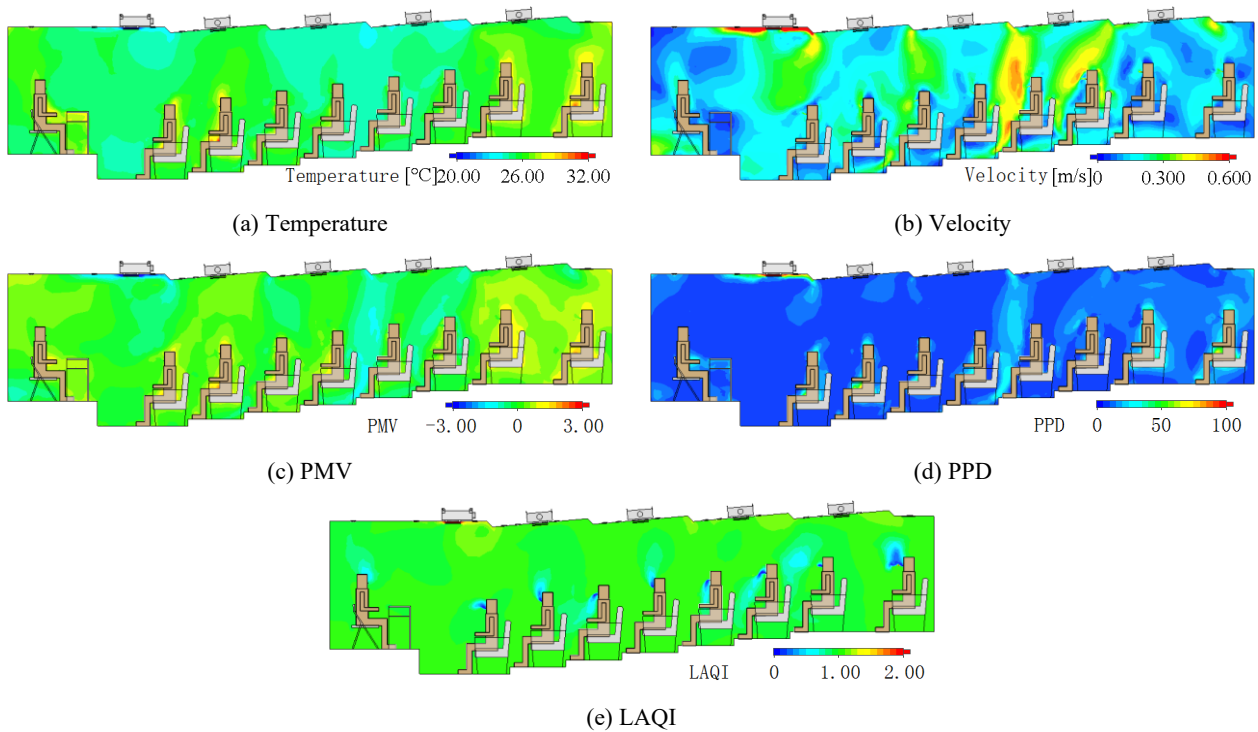


Figure 7. Mixed ventilation ($x=2.3\text{ m}$).

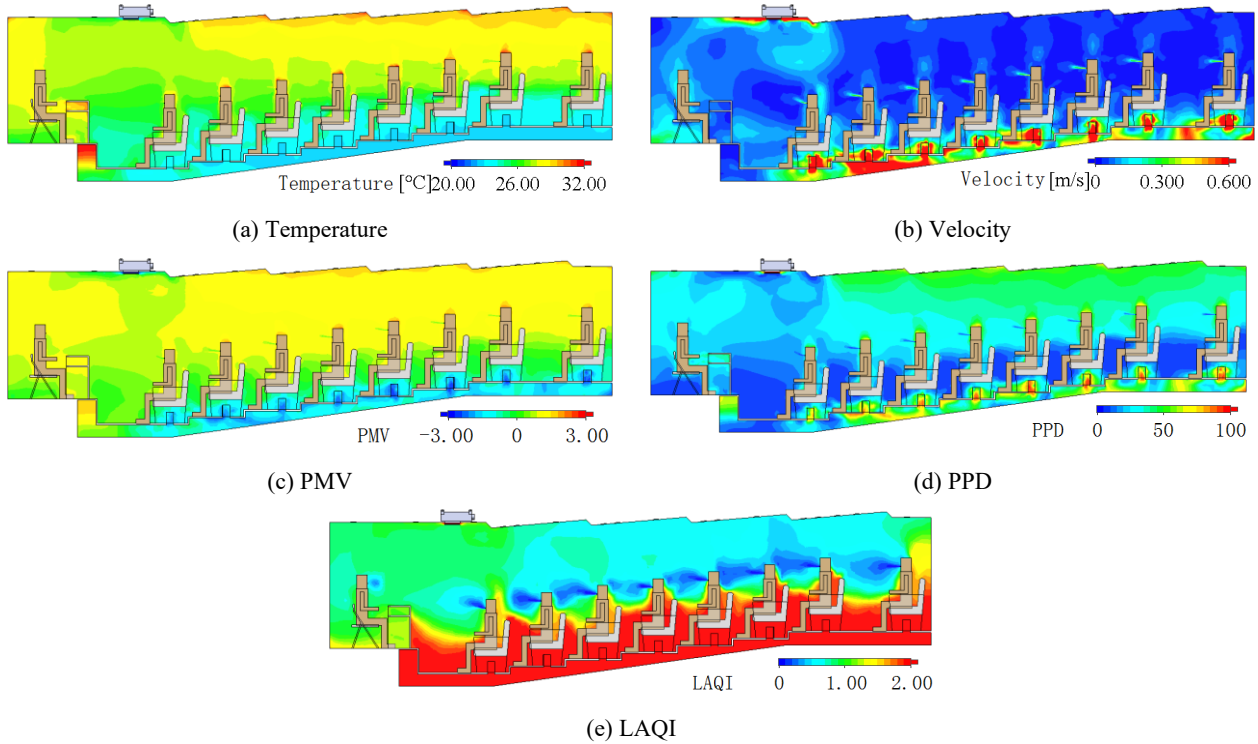


Figure 8. Displacement ventilation ($x=2.3$ m).

Figures 7 and 8 show the air characteristic contours at $x=2.3$ m section for mixed and displacement ventilation, respectively. The average temperature of mixed ventilation is 25.6°C , and its temperature distribution has good uniformity in the whole cabin, with an average airflow velocity of 0.15 m/s. In the middle of the cabin, due to the convergence of the airflow of the air distributor, there is a local area with high air velocity; the average temperature of displacement ventilation is 25.9°C , and its airflow organization has apparent air stratification phenomenon, and the top area temperature is higher than that of the occupied zone, with an average airflow velocity of 0.08 m/s. All areas except the area near the seat air supply column have very low air velocity.

Table 2 shows the ventilation comfort indicators of the occupied zone for the two schemes. According to the relevant standards, the comfort indexes in the cabin should satisfy $-0.5 < PMV < 0.5$, $PPD < 10\%$, and $PD < 5\%$ ¹⁷. Each thermal comfort index of the mixed ventilation can meet the requirements, and the contaminant removal effectiveness is 1. The displacement ventilation scheme, due to the insufficient floor height and the unreasonable setting of the exhaust outlet, resulted in a low thermal stratification height. The thermal stratification height overlaps with the personnel activity zone, and the $PPD=18.5\%$ within the personnel activity zone does not meet the requirements. The PD at each row of seats is given in Figure 9, which shows that Although the $PD=3.0\%$ within the personnel activity zone, the PD values at the first and sixth rows of seats are close to the upper limit or unsatisfactory. The $CRE=1.04$, which is not significantly improved compared to the mixed ventilation, it can be seen from Figure 8e that although the CRE close to the floor is close to 2, the values near the breathing range of the personnel are lower compared to the mixed ventilation.

Table 2. Ventilation comfort indexes.

Design scheme	Temperature/ $^{\circ}\text{C}$	Velocity/m/s	PMV	$PPD/\%$	$DR/\%$	$PD/\%$	CRE
Mixed ventilation	25.6	0.15	0.21	9.0	6.8	0.4	1.00
Displacement ventilation	25.9	0.08	0.49	18.5	3.5	3.0	1.04

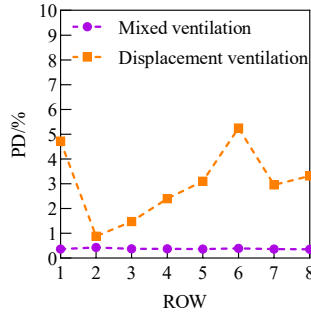


Figure 9. Percentage of vertical temperature difference dissatisfied.

From the above computation results and analysis, it can be seen that the thermal comfort and contaminant removal effectiveness in the original displacement ventilation scheme is poor due to the low height of the thermal stratification, which needs to be optimized and improved, as shown in Figure 10. In the optimization scheme, the exhaust grille at the top of the last row of seats is eliminated, and the four short beveled edges of the ceiling are changed into exhaust/return grilles.

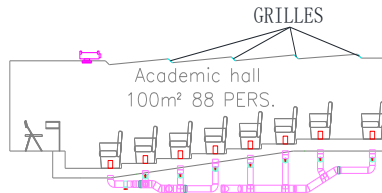


Figure 10. Optimized displacement ventilation.

Figures 11 and 12 show the air characteristic cloud diagrams at sections $x=2.3$ m and $x=4.6$ m of the optimized displacement ventilation. It can be seen that the optimized displacement ventilation effectively increases the height of the thermal stratification, and the cabin temperature gradient is significantly decreased compared to the original displacement ventilation. The optimization maintains the average air velocity at 0.08 m/s while lowering the average temperature to 25.6°C compared to the original displacement ventilation.

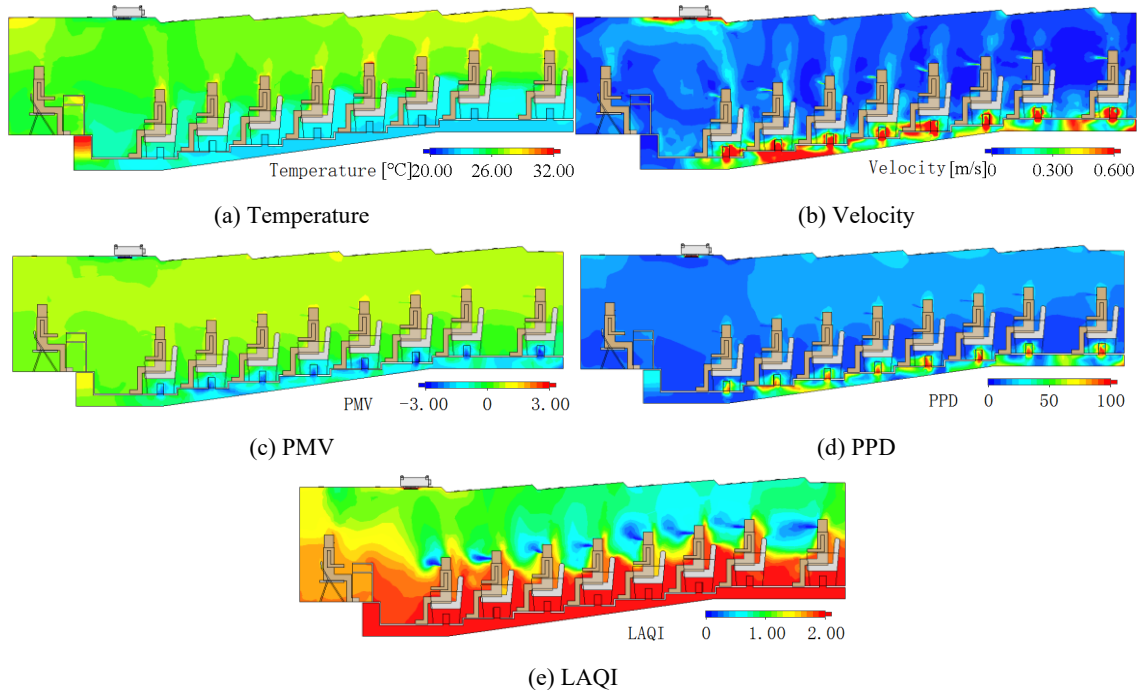


Figure 11. Optimized displacement ventilation ($x=2.3$ m).

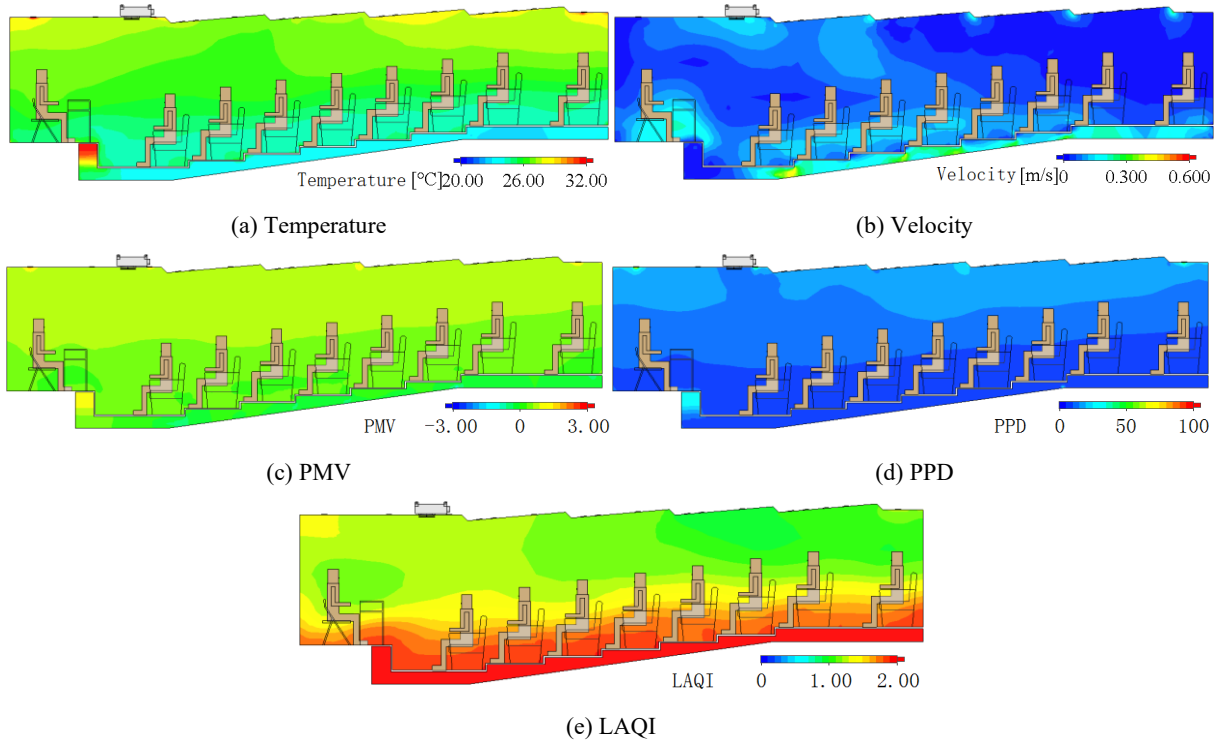


Figure 12. Optimized displacement ventilation ($x=4.6$ m).

Table 3 shows the comfort indices of ventilation in the occupied zone for the optimized displacement ventilation. Each comfort index is also better than the original displacement ventilation, especially the *CRE*, which is significantly improved to 1.95, and the rising airflow sufficiently carries the contaminants away from the occupied zone. The *PD* at each row of seats is given in Figure 13, and the values at each row of seats met the standard requirements.

Table 3. Ventilation comfort indexes.

Design scheme	Temperature/°C	Velocity/m/s	PMV	PPD/%	DR/%	PD/%	CRE
Optimized displacement ventilation	25.6	0.08	0.41	9.8	3.4	1.7	1.95

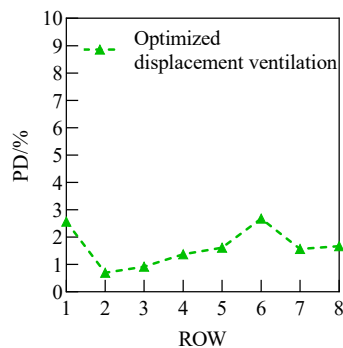


Figure 13. Percentage of vertical temperature difference dissatisfied.

Four measurement points were set up in the academic hall, and the locations of measurement points 1 ($x=4.6$ m, $y=3.5$ m), 2 ($x=4.6$ m, $y=5.5$ m), 3 ($x=4.6$ m, $y=7.5$ m), and 4 ($x=2.3$ m, $y=5.5$ m) are shown in Figure 3a. The curves of dimensionless temperature, dimensionless velocity, and *LAQI* with height at each measurement point are shown in Figure 14. It can be seen that the air temperature near the floor rises due to induction, convection, and radiation from other hot surfaces in the cabin, and the temperature rise at the floor accounts for about half of the difference between the

supply and exhaust air temperatures, but the other half is not distributed linearly in the altitude direction, with a more significant temperature gradient in the occupied zone and a smaller temperature gradient in the top area. As the air supply column of the seat directly sends air to the occupied zone, the air velocity of the whole cabin near the floor is higher than in other areas. However, due to the low velocity of the supply air, the overall air velocity is also kept at a low level, which can effectively avoid the draft. The contaminant removal effectiveness in the occupied zone is higher than in the top area, ensuring that the personnel breathe clean air. Because the contaminants are continuously released when the human body breathes in the computation, the *CRE* in part of the range of measurement point 4 is relatively low, and the *CRE* should be better than the calculated value in the actual situation.

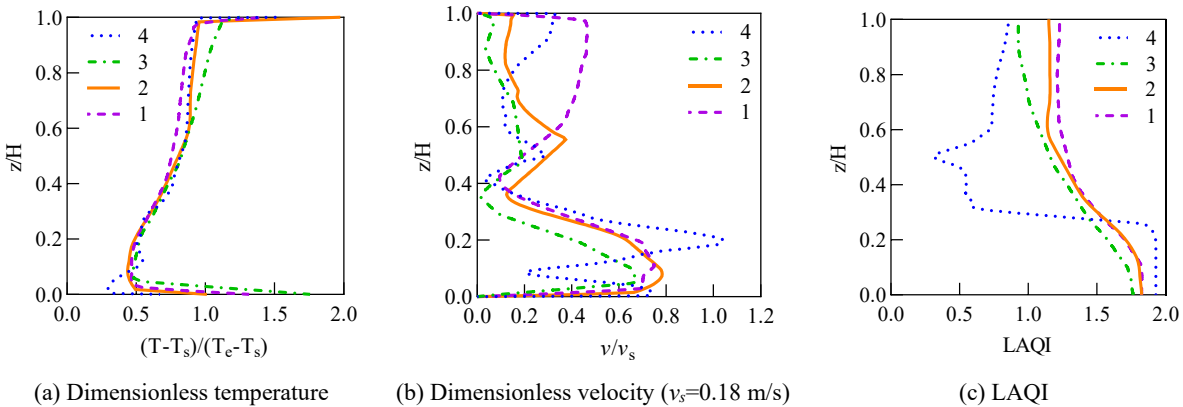


Figure 14. Profiles of air properties with height at different measurement points.

5. CONCLUSIONS

In this paper, a comparative validation of CFD methods was first carried out for a displacement ventilation experimental compartment, followed by a numerical simulation study on the airflow organization of a ship's cabin under different ventilation modes, and the results show that:

- (1) The CFD method and model described in this paper can effectively solve the displacement ventilation problem;
- (2) Displacement ventilation has the characteristics of flow stratification, vertical temperature gradient, low draft sensation, and better contaminant removal effectiveness than mixed ventilation, *CRE* is 1.95 times higher than that of mixed ventilation, the air supply temperature is 1.5°C higher than that of mixed ventilation so that the air-conditioning load can be reduced by 15%, which ensures that the thermal comfort indices of the occupied zone are in line with the standard requirements and the contaminants can be effectively removed;
- (3) Theoretical methods carry out the preliminary design of displacement ventilation, and then CFD method is used to verify that a better design effect can be obtained and that displacement ventilation can be used in ship cabins with low floor heights and dense personnel after reasonable design.

This paper's computation and analysis results provide a reference for designing and optimizing different ventilation modes in ship cabin.

REFERENCES

- [1] Kim, S. S. and Lee, Y. G., "Field measurements of indoor air pollutant concentrations on two new ships," *Building and Environment*, 45(10), 2141-2147 (2010).
- [2] Acar, A., Uryan, M., Doğrul, A., Karakurt, A. S., et al. "Numerical investigation of HVAC systems of a naval ship compartment: natural ventilation and air-conditioning," *Journal of Naval Sciences and Engineering*, 19(1), 77-100 (2023).
- [3] Shi, H., Zhang, Q., Xu, W., Liu, M., Pan, J., Yuan, J. and Yang, K. "Optimization of cockpit ventilation for polar cruise ships in combination with windscreen defogging and cabin comfort considerations," *Entropy*, 24(8), 1061 (2022).

- [4] Zhang, S., Gao, H., Lin, Z., Zhao, Y., Guo, Y. and Hu, Y., “Numerical simulation and analysis of air supply mode in luxury cruise air-conditioning system,” *Journal of Physics: Conference Series*, 2029(1), 012119 (2021).
- [5] Khalil, E. E., “Thermal comfort and airflow patterns in cruise ships,” *AIAA Propulsion and Energy 2020 Forum*, 3940 (2020).
- [6] Sun, L., Tan, S. and Liu, L., “Influence of air supply mode on airflow distribution in ship conference room applying cooling ceiling,” *Science and Technology for the Built Environment*, 23(8), 1293-1304 (2017).
- [7] Liu, H., “Simulation and optimization of indoor thermal environment in a ship air-conditioning system,” *Procedia Environmental Sciences*, 11, 1055-1063 (2010).
- [8] Handbook, A. S. H. R. A. E., “Heating, ventilating, and air-conditioning applications.” *American Society of Heating, Refrigerating and Air Conditioning Engineers*, (2011).
- [9] Patankar, S., “Numerical heat transfer and fluid flow,” *CRC press*, (2018).
- [10] Fanger, P. O., “Thermal comfort: analysis and applications in environmental engineering,” *RE Krieger Pub. Co.: Malabar, FL, USA*, (1982).
- [11] ISO 7730, “Moderate thermal environments. Determination of the PMV and PPD indexes and specification of the conditions for thermal comfort,” (2005).
- [12] Skistad, H., Mundt, E., Nielsen, P. V., Hagström, K., and Railio, J., “Displacement ventilation in non-industrial premises,” *REHVA*, (2002).
- [13] Chen, Q., Glicksman, L. R., Yuan, X., Hu, S., Hu, Y. and Yang, X., “Performance evaluation and development of design guidelines for displacement ventilation,” *Draft Final Report to ASHRAE TC*, 5 (1999).
- [14] Li, Y., Sandberg, M. and Fuchs, L., “Vertical temperature profiles in rooms ventilated by displacement: full-scale measurement and nodal modelling,” *Indoor Air*, 2(4), 225-243 (1992).
- [15] Li, Y., Sandberg, M. and Fuchs, L., “Effects of thermal radiation on airflow with displacement ventilation: an experimental investigation,” *Energy and buildings*, 19(4), 263-274 (1993).
- [16] ISO 7547, “Ships and marine technology. Air-conditioning and ventilation of accommodation spaces. Design conditions and basis of calculations” (2022).
- [17] Standard, A. S. H. R. A. E., “Standard 55-2023, Thermal environmental conditions for human occupancy,” *American Society of Heating, Refrigerating and Air Conditioning Engineers*, (2023).